Journal of Orthopaedic Translation 48 (2024) 39–52

Contents lists available at ScienceDirect

Journal of Orthopaedic Translation

journal homepage: www.journals.elsevier.com/journal-of-orthopaedic-translation

Mechanical loading on osteocytes regulates thermogenesis homeostasis of brown adipose tissue by influencing osteocyte-derived exosomes

Yuze Ma [a], Na Liu [b], Xiaoyan Shao [b], Tianshu Shi [a], Jiaquan Lin [b], Bin Liu [a], Tao Shen [a], Baosheng Guo [b,*], Qing Jiang [a,**]

[a] *Division of Sports Medicine and Adult Reconstructive Surgery, Department of Orthopedic Surgery, Nanjing Drum Tower Hospital, Affiliated Hospital of Medical School, Nanjing University, Nanjing, China*

[b] *Jiangsu Key Laboratory of Molecular Medicine, Medical School, Nanjing University, Nanjing, Jiangsu, China*

ARTICLE INFO

Keywords:
BAT
Exosome
miRNA
Osteocyte
Thermogenesis

ABSTRACT

Background: Osteocytes are the main stress-sensing cells in bone. The substances secreted by osteocytes under mechanical loading play a crucial role in maintaining body homeostasis. Osteocytes have recently been found to release exosomes into the circulation, but whether they are affected by mechanical loading or participate in the regulation of systemic homeostasis remains unclear.

Methods: We used a tail-suspension model to achieve mechanical unloading on osteocytes. Osteocyte-specific CD63 reporter mice were used for osteocyte exosome tracing. Exosome detection and inhibitor treatment were performed to confirm the effect of mechanical loading on exosome secretion by osteocytes. Co-culture, GW4869 and exosome treatment were used to investigate the biological functions of osteocyte-derived exosomes on brown adipose tissue (BAT) and primary brown adipocytes. Osteocyte-specific Dicer KO mice were used to screen for loading-sensitive miRNAs. Dual luciferase assay was performed to validate the selected target gene.

Results: Firstly, we found the thermogenic activity was increased in BAT of mice subjected to tail suspension, which is due to the effect of unloaded bone on circulating exosomes. Further, we showed that the secretion of exosomes from osteocytes is regulated by mechanical loading, and osteocyte-derived exosomes can reach BAT and affect thermogenic activity. More importantly, we confirmed the effect of osteocyte exosomes on BAT both in vivo and in vitro. Finally, we discovered that let-7e-5p contained in exosomes is under regulation of mechanical loading and regulates thermogenic activity of BAT by targeting *Ppargc1a*.

Conclusion: Exosomes derived from osteocytes are loading-sensitive, and play a vital role in regulation on BAT, suggesting that regulation of exosomes secretion can restore homeostasis.

The translational potential of this article: This study provides a biological rationale for using osteocyte exosomes as potential agents to modulate BAT and even whole-body homeostasis. It also provides a new pathological basis and a new treatment approach for mechanical unloading conditions such as spaceflight.

1. Introduction

The skeletal system constitutes approximately 15 % of the total body weight and represents one of the largest organs in the human body [1]. In the past, bones were primarily perceived as providing structural and movement support; however, in recent years, there has been an increasing recognition of the pivotal role that bones play in maintaining homeostasis within the body [2]. Osteocytes, comprising more than 90 % of bone cells, are recognized as pivotal cellular components within this tissue [3]. These specialized cells possess an exceptional ability to perceive and respond to mechanical stimuli exerted upon bones [4]. Previous studies have demonstrated that osteocytes possess the ability to secrete proteins, such as sclerostin, which subsequently exert regulatory effects on distal target organs including muscle, liver, and brain [5,6]. Furthermore, this endocrine function is modulated in response to stress stimulation. Recent discoveries have unveiled that osteocytes release

* Corresponding author.
** Corresponding author.
E-mail addresses: borisguo@nju.edu.cn (B. Guo), qingj@nju.edu.cn (Q. Jiang).

https://doi.org/10.1016/j.jot.2024.06.012
Received 16 January 2024; Received in revised form 25 May 2024; Accepted 19 June 2024

exosomes [7,8]. Exosomes, ranging in diameter from 30 to 150 nm, play a crucial role in intercellular communication by facilitating the transfer of functional proteins, metabolites, and nucleic acids to recipient cells across both short and long distance [9]. For instance, miR-181b-5p encapsulated within osteocyte-derived exosomes regulates proliferation and osteogenic differentiation of human periodontal ligament stem cells [7]; while miR-483-3p and miR-513a-5p derived from exosomes secreted by osteocytes confer chemoresistance upon myeloma cells [10]. However, thus far only short-range regulatory effects mediated by osteocyte exosomes have been elucidated with their influence on distal tissues or organs remaining unclear.

BAT is a distinct type of adipose tissue that differs from white adipose tissue in its energy storage properties [11]. It achieves non-shivering thermogenesis through the key protein UCP1 and plays a role in maintaining body homeostasis [11]. Since physical exercise can profoundly affect body homeostasis, the association between musculoskeletal System and BAT has attracted growing attention in recent years. Researchers have made the discovery that BAT has the capability to release myostatin and 12,13-diHOME, thereby exerting regulatory effects on muscle function [12,13]. Also, exercise-induced release of myokines promotes browning of adipocytes to stimulate thermogenesis [14,15]. While the interaction between BAT and muscle is well-established, the interplay between BAT and bone remains poorly understood. Only a few studies have reported on the impact of BAT on bone health so far [16,17]. Interestingly, some researchers found that thermogenic markers of BAT were altered both in mice during space flight [18] and rats subjected to tail suspension [19]. Considering that the mechanical loading is the vital fact at the situation mentioned above, osteocytes, as the main stress-sensing cells in bone, may play a regulatory role on BAT.

In the current study, we investigated the mechanisms underlying osteocyte-mediated communication with BAT. Initially, we observed that mechanical unloading of osteocytes led to an upregulation of thermogenic activity in BAT. Subsequently, we identified that mechanical loading triggered calcium influx and then activated the CAMKII/CREB signaling pathway, thereby influencing exosome secretion from osteocytes. Additionally, our findings revealed that let-7e-5p, a miRNA sensitive to mechanical loading, was encapsulated within osteocyte-derived exosomes and remotely regulated the thermogenic activity of BAT by targeting *Ppargc1a*. Furthermore, we emphasize the role of stress-mediated osteocyte exosomes in modulating whole-body homeostasis.

2. Methods

2.1. Animal experiments

The C57BL/6 male mice were purchased from Nanjing Ziyuan Biotechnology Co. Ltd (Nanjing, China). The animal experiments were conducted according to the Institutional Animal Ethics Committee and Animal Care Guidelines for the Care and Use of Laboratory Animals of Nanjing University. The mice were provided with ad libitum access to food and water. Mice were kept in cages under standard laboratory conditions with a 12-h dark, 12-h light cycle. According to the previous study [20], a key ring was affixed to one end of the bar and secured to the mouse's tail using tape at the other end. The vertical position was adjusted to incline the mouse's head approximately 30° downward. Each cage was inhabited by a single mouse. For cold resistance experiments, mice were kept at 4 °C and rectal temperature was measured as core body temperature at hourly intervals.

Dicer cKO mice were generated by crossing Dmp1-Cre mice with Dicer$^{flox/flox}$ mice. For osteocyte-specific exosome reporter mice, CD63-GFP$^{flox/+}$ and Dmp1-Cre mice were bred to generate Dmp1-Cre; CD63-GFP$^{flox/+}$ mice.

The adeno-associated virus (AAV) loaded with mmu-let-7e-5p were synthesized and constructed by OBiO Technology (Shanghai) Corp., Ltd. The BAT of mice were injected with 30 μl AAV (10^{11}), and the BAT were collected for further investigation 1-month post-injection.

2.2. Cell culture experiments

Mouse MLO-Y4 osteocytes were obtained from ATCC and cultured in AMEM containing 5 % fetal bovine serum (FBS, Gibco), 5 % calf Serum (CS, Gibco) and 1 % penicillin–streptomycin. For miRNA transfection, primary brown adipocytes were seeded into 12-well or 6-well plates and reached to 70–80 % confluency. Then primary brown adipocytes were transfected with either mmu-let-7e-5p mimic (Ribo, Guangzhou, China) at 50 nmol/mL, mmu-let-7e-5p inhibitor (Ribo, Guangzhou, China) at 100 nmol/mL, or negative control using Lipofectamine 2000 (Invitrogen, Guangzhou, China). After 6–8 h, the culture medium was replaced with culture medium, followed by browning differentiation. Luciferase reporter plasmids containing the WT or mutant 3′-UTR of *Ppargc1a* were manufactured by Hanheng Biotechnology (Shanghai, China). The 293T cells were used for the luciferase reporter assays.

For mechanical loading experiments, osteocytes were cultured on six-well Biofex plates (Flexcell). At 90 % confluence, cells were serum starved in α-MEM for 24 h and were then subjected to mechanical loading (5 %, 0.5 Hz) for 24 h. As static controls, cells were seeded into the same kind of plates but were not subjected to mechanical loading. While exposed to mechanical loading, osteocytes were treated with GdCl3 (60 μM), or KN-93 (10 μM), or 666-15 (1 μM) as experimental groups accordingly [21–23], and osteocytes with no treatment serves as control group.

2.3. Isolation, culture and co-culture of bone tissue

The bone tissue was isolated and cultured as previously described [24,25]. First, the lower limb bones were dissected aseptically. Subsequently, the bone marrow cavity was flushed with PBS. The bones were then segmented into fine bone fragments and enzymatically digested with type I collagenase, repeating this process three times for 20–30 min each. This was followed by alternating digestion with EDTA solution and type I collagenase for 20–30 min and repeated three times. Ultimately, the bone fragments were subjected to washing and cultured in AMEM with 10 % FBS. For the co-culture experiment, the bone fragments were cultured on the lower layer, while the primary brown adipocytes were cultured on the transwell chambers during differentiation.

2.4. Isolation and differentiation of primary brown adipocytes

Mouse primary brown adipocytes were isolated from BAT of newborn mice within 2 days of birth according to previous studies [26,27]. In brief, BAT was dissected and digested with 0.1 % collagenase for 30 min. The resulting suspension was filtered and the filtrate was centrifuged at 300g. The supernatant was subsequently discarded, and the cultures were resuspended in DMEM, containing 10 % FBS and 1 % penicillin–streptomycin.

For the browning differentiation experiment, when confluence was reached to 100 % for 2 days, primary brown adipocytes were induced with browning differentiation medium (DMEM with 10 % FBS, 1 % penicillin–streptomycin, 1 μM rosiglitazone, 0.5 mM IBMX, 1 μM dexamethasone, 200 nM insulin, 10 nM T3, and 125 μM Indomethacin). Two days after induction, cells were re-fed every 48 h with browning culture medium containing 1 μM rosiglitazone, 200 nM insulin and 10 nM T3. Cells were fully differentiated by day 5 after induction [27,28].

2.5. Isolation and labeling of exosomes

Exosomes were purified from the cultured supernatants or plasma using a previously described method [29]. Briefly, supernatants were collected and centrifuged at 300g for 10 min, followed by centrifugation at 2,000g, for 10 min and 10,000g for 30 min for removal of large vesicles. Then, the supernatants were centrifuged at 100,000g for 100 min. The pelleted exosomes were collected and resuspended in PBS. To monitor exosomes trafficking, exosomes were labeled with PKH26 fluorescent dye using a PKH26 fluorescence cell linker kit (Sigma–Aldrich). After staining, the exosomes were washed with PBS and collected via ultracentrifugation. Finally, PKH26-labeled exosomes were resuspended in PBS.

2.6. In vitro and in vivo exosome treatment

In vitro, exosomes were co-cultured with primary brown adipocytes, and the culture medium containing exosomes was changed every 2 days. In vivo, 30 μL PBS containing 100 μg of exosomes was locally injected into BAT twice per week.

2.7. In vivo GW4869 treatment

For the in vivo GW4869 treatment, we employed a bone-targeted delivery approach [30]. Specifically, the lipid nanoparticle (LNP) composed of DSPE-PEG_{2000} was conjugated with repetitive sequences of aspartate, serine, serine. GW4869 is effectively encapsulated within the LNP. The drug, GW4869@DSPE-PEG_{2000}-MAL-$(DSS)_6$, was injected twice a week via the tail vein (2.5 ug/g body weight).

2.8. Gene expression analysis

Total RNA was extracted using TRIzol (Invitrogen). Total RNA was reverse transcribed into cDNA following the manufacturer's protocol. The expression of mature miRNAs was detected by a Hairpin-it miRNA and U6 normalization Q-PCR Quantitation Kit (Ribo, Guangzhou, China), and the primers for miRNAs were obtained from Ribo (Guangzhou, China). Real-time qPCR was performed with the ChamQ SYBR qPCR Master Mix (Vazyme, Nanjing, China). Gene expression was normalized to that of β-actin.

2.9. Immunoblot analysis

Tissue samples or cell samples were homogenized in RIPA buffer (Thermo Fisher Scientific) containing protease and phosphatase inhibitors. Total proteins were boiled at 99 °C for 5 min after adding the 5 × SDS-PAGE protein loading buffer (BOSTER, China). For western blotting, after electrophoresis on SDS-PAGE gels, the proteins were transferred to PVDF membranes and incubated for 1 h in blocking buffer. The membranes were then incubated overnight with primary antibodies, followed by incubation with a horseradish peroxidase (HRP)-conjugated secondary antibody. Detected proteins were quantified by densitometry using NIH Image J software.

2.10. Staining

The BAT were dehydrated and embedded in paraffin, and then cut into sections for H&E staining. For immunohistochemistry (IHC) staining, the sections were performed as described and then incubated with primary antibodies. The sections were incubated with secondary antibodies the following day. For immunofluorescence, the BAT were dehydrated in a mixture of 30 % sucrose phosphate buffer, and then embedded in optimum cutting temperature (O.C.T., Fisher Healthcare). Immunofluorescence staining was performed as described and the sections were incubated overnight with primary antibodies. The sections were incubated with the appropriate secondary antibodies. Nuclei were counterstained with DAPI (Beyotime, China).

2.11. Micro-CT analysis

The femurs of mice in each group were fixed in 4 % PFA and scanned by SCANCO vivaCT 80 (MedicalAG). We assessed trabecular bone microstructure in the distal femur. Morphometric variables were computed from the binarized images using direct, 3D techniques. We assessed the bone volume fraction (BV/TV), trabecular bone mineral density (BMD, mg HA/cm^3), trabecular thickness (Tb.Th, mm), trabecular number (Tb.N, mm^{-1}), trabecular separation (Tb.Sp, mm), structural mode index (SMI) and connectivity density (Conn.D., mm^{-3}).

2.12. Statistics analysis

Data are presented as means ± SD. Statistical analysis was performed using unpaired Student's t-tests. Statistical analyses were performed with GraphPad Prism software. P values < 0.05 were considered to be statistically significant.

3. Results

3.1. Mechanical unloading of bone tissue may enhance the thermogenic activity of BAT by modulating circulating exosomes

To achieve mechanical unloading of bone tissue, the mice were subjected to a 4-week tail suspension treatment as tail suspension (TS) group, while the mice of control (CTR) group were not treated. We recorded the body weight of the mice before and after tail suspension (Fig. S1A). Mice showed weight loss after experiencing tail suspension compared to controls. Micro CT analysis of the mouse skeletal system revealed a significant decrease in bone density and notable changes in skeletal microstructure (Fig. 1A), confirming successful modeling through 4 weeks of tail suspension. At the end of the experiment, mice were exposed to a temperature of 4 °C and rectal temperature was measured every hour as an indicator of core body temperature. The results showed that mice of TS group exhibited higher core body temperatures at the 3rd and 4th hour (Fig. 1B), indicating enhanced cold resistance capabilities. To further investigate this phenomenon, we examined relevant thermogenic indicators of BAT. Our findings demonstrated that compared to the CTR group, the transcript level of *Ucp1* was significantly higher in BAT of TS group (Fig. 1C). Correspondingly, protein expression levels associated with BAT thermogenesis were also higher in this group (Fig. 1D). Additionally, images of H&E staining revealed smaller lipid vacuoles and denser tissue structure within BAT of TS group (Fig. 1E); images of IHC staining confirmed increased UCP1 expression as well (Fig. 1F). These results provide evidence that mice treated with tail suspension exhibit stronger cold resistance due to heightened thermogenic activity of BAT.

Studies have shown that bone tissue, as an endocrine organ, secrets substances involved in homeostasis regulation under a variety of physiological and pathological conditions [2]. Building upon findings above, we propose that bone tissue may exert a regulatory role in the thermogenic activity of BAT. To verify this hypothesis, we isolated bone tissue from mice of TS group and CTR group and co-cultured it with primary brown adipocytes. Our results revealed that compared to the CTR group, bone tissue from tail-suspended mice significantly enhanced the thermogenic activity of primary brown adipocytes. The transcript levels of *Ucp1*, *Ppargc1a*, *Prdm16*, *Pparg*, and *Cebpb* were all upregulated in the primary brown adipocytes co-cultured with bone tissue of TS group (Fig. 1G). Additionally, protein expression level of UCP1 was also increased (Fig. 1H). Consistent with these findings, conditioned medium derived from bone tissue of TS group exhibited an ability to enhance the thermogenic activity of primary brown adipocytes (Figs. S1B and S1C). Furthermore, to mimic mechanical loading on bone tissue similar to its physiological condition in vivo, we employed a Flexcell system to apply mechanical loading on MLO-Y4, a cell line of osteocytes. Since bone tissue from TS group experienced minimal mechanical loading, the TS group corresponded to unloading group in vitro experiments while CTR group corresponded to loading group. The results obtained from in vitro experiments were consistent with those obtained in vivo (Figs. S1D and S1E). These results suggest that unloaded bone induces enhanced thermogenic activity in brown adipocytes.

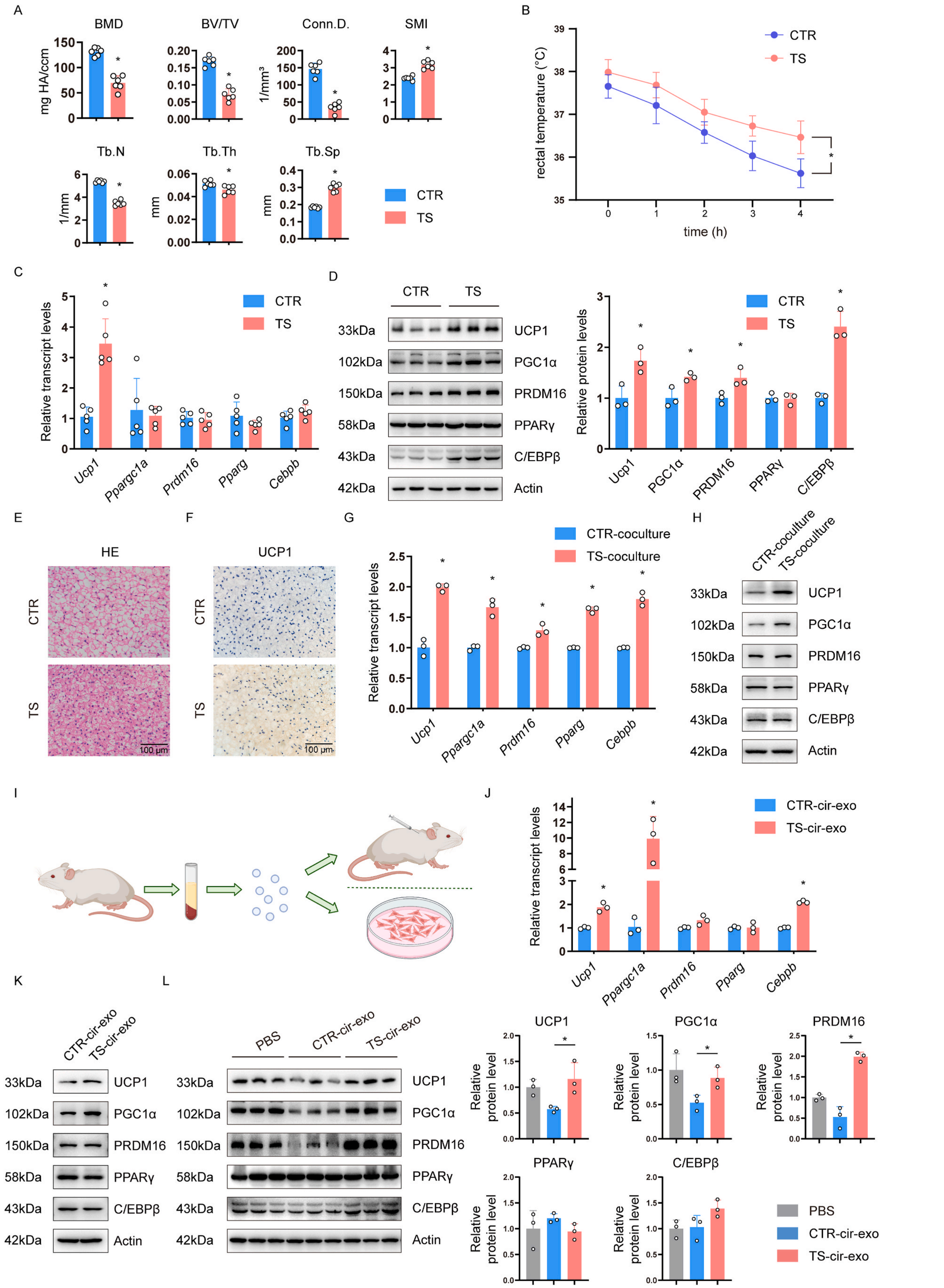

(caption on next page)

Fig. 1. Mechanical unloading of bone tissue may enhance the thermogenic activity of BAT by modulating circulating exosomes. Mice were subjected to tail suspension (TS group) or not (CTR group) for 4 weeks. N = 6. (A–F) (A) Micro-CT analysis of distal femur. (B) Core body temperature of mice exposed to 4 °C. (C) Transcript levels of thermogenic genes in BAT. (D) WB analysis and relevant quantification analysis of thermogenic proteins in BAT. (E) Representative H&E staining images of BAT. (F) Representative IHC staining images of BAT. (G) Transcript levels of thermogenic genes and (H) WB analysis of thermogenic proteins were performed on primary brown adipocytes co-cultured with ex vivo bone tissue from both CTR and TS group. (I) A diagram depicts the isolation of circulating exosomes from mouse plasma, followed by their local injection into BAT or treatment on cells. (J) Transcript levels of thermogenic genes and (K) WB analysis of thermogenic proteins were performed on primary brown adipocytes treated with circulating exosomes. (L) WB analysis of thermogenic proteins were performed on BAT following local injection with circulating exosomes. All data are Mean ± SD. *P < 0.05. (For interpretation of the references to color in this figure legend, the reader is referred to the Web version of this article.)

To further investigate how bone tissue affect the thermogenesis activity of BAT remotely, we extracted plasma exosomes from mice (Figs. S1F–H), and treated cells or BAT with exosomes (Fig. 1I). No significant difference was observed in the number of exosomes between the two groups (Figs. S1I and S1J). We treated primary brown adipocytes with the same amount of plasma exosomes, and found that plasma exosomes from TS group induced increased gene transcription and protein expression of *Ucp1* and *Ppargc1a* in vitro (Fig. 1J and K). Subsequently, plasma exosomes were locally injected into mouse BAT to evaluate their direct effects. Consistent with our findings in vitro, treatment with plasma exosomes derived from mice of TS group induced elevated protein expression of UCP1, PGC1α, and PRDM16 in vivo (Fig. 1L). The finding above indicate that circulating exosomes derived from TS group can enhance the thermogenic activity of BAT.

3.2. Mechanical unloading causes a decrease in the release of exosomes from osteocytes

Since both plasma exosomes and bone tissue derived from TS group could increase the thermogenic activity of BAT, we hypothesized that mechanical loading affect the secretion of exosomes from bone tissue, thereby modulating BAT thermogenesis via plasma exosomes. To investigate this, we generated Dmp1-cre; CD63-GFP$^{flox/+}$ mice for specific tracking of osteocyte-derived exosomes (Fig. 2A). Our findings revealed a decrease in osteocyte CD63 expression in TS group (Fig. 2B), indicating reduced exosomes derived from osteocytes due to unloading. Furthermore, PKH26 staining and statistical analysis demonstrated a decreased proportion of osteocyte-derived exosomes (Fig. S2A), further supporting diminished release into circulation by osteocytes under unloading conditions.

To obtain more direct evidence of exosome secreted by osteocytes, bone tissue was isolated and cultured, and the bone-culture supernatant was collected to extract the secreted exosomes. Consistent with the aforementioned findings, we observed a decrease in exosome secretion from bone tissue in the TS group compared to the CTR group (Fig. 2C). Furthermore, we detected Rab27a expression as it is known to play a crucial role in regulating exosome secretion [31]. Our results demonstrated decreased transcript and protein expression level of Rab27a in bone tissue of TS group following mechanical unloading treatment (Fig. 2D and E). Representative images of IHC staining and IF staining confirmed reduced Rab27a expression specifically in osteocytes after mechanical unloading within the bone tissue of the TS group (Fig. 2F and G). Additionally, we examined the effect of loading on osteocyte-mediated exosome secretion in vitro and found that loaded osteocytes exhibited increased exosome release compared to unloaded osteocytes (Fig. 2H), corresponding to the TS group which showed reduced exosome secretion. These findings align with our in vivo study where lower transcript and protein expression level of Rab27a were observed in unloaded osteocytes (Fig. 2I and J). Additionally, CD63-GFP signal intensity in BAT from mice suggested reduced delivery of osteocyte-derived exosomes to BAT during mechanical unloading (Fig. 2K). Collectively, these results suggest that mechanical unloading diminishes exosome secretion by suppressing osteocyte-specific Rab27a expression, consequently impairing normal regulation exerted by osteocytes on BAT.

3.3. Mechanical loading modulates exosome secretion by osteocytes via the CAMKII/CREB signaling pathway

Previous studies have demonstrated that osteocytes undergo calcium influx and phosphorylation of CAMKII in response to mechanical loading [22,32]. Additionally, it has been found that CREB, a downstream protein of CAMKII, regulates the expression of Rab27a [33–35]. Based on these findings, we propose that mechanical loading regulates the secretion of osteocyte exosomes by inducing calcium influx and activating the CAMKII/CREB pathway. To investigate this hypothesis, we initially examined the intracellular calcium level after subjecting osteocytes to mechanical loading and observed a significant increase in intracellular calcium level (Fig. 3A). Furthermore, we observed an upregulation in the phosphorylation levels of both CAMK2A and CREB (Fig. 3B), which aligns with our hypothesis. To determine if calcium influx was responsible for these effects, we treated osteocytes with $GdCl_3$ to block calcium influx subsequent to mechanical loading. Our results showed that $GdCl_3$-treated osteocytes exhibited lower intracellular calcium level as well as reduced phosphorylation levels of CAMK2A and CREB compared to control group subjected only to mechanical loading (Fig. 3C and D). These findings suggest that calcium influx plays a crucial role in promoting increased phosphorylation of CAMK2A and CREB. Moreover, analysis indicated decreased gene expression and protein level of Rab27a in the $GdCl_3$ treatment group (Fig. 3D and E), further supporting our conclusion that mechanical stimulation-induced calcium influx contributes to regulation of Rab27a expression. Additionally, the concentration of exosomes decreased post-treatment as anticipated (Fig. 3F).

To further elucidate the involvement of CAMKII in regulating exosome secretion, loaded osteocytes were treated with KN-93, a reversible and competitive inhibitor of CAMKII that impairs phosphokinase function [22]. Our findings indicate that phosphorylation of CREB was attenuated following KN-93 treatment (Fig. 3G), suggesting the role of CAMK2A's phosphokinase activity in loading-induced increase in CREB phosphorylation. The reduced phosphorylation level of CAMK2A may be attributed to its impaired ability of autophosphorylation. Moreover, downregulation of Rab27a protein expression and decreased exosome concentration were observed (Fig. 3G and H), indicating the contribution of CAMK2A's phosphokinase activity to loading-induced exosome secretion. These results highlight the involvement of CAMK2A's phosphokinase activity in regulating Rab27a expression and exosome release via CREB phosphorylation under mechanical loading. Finally, we employed 666-15, a potent inhibitor targeting CREB-mediated gene transcription [23], to elucidate the pivotal role of CREB in governing Rab27a transcription. Treatment with 666-15 resulted in decreased transcript level and protein expression level of Rab27a (Fig. 3I and J), and reduced exosome concentration (Fig. 3K), providing evidence for the involvement of CREB-mediated transcriptional regulation in exosome release from osteocytes. Collectively, our findings suggest that mechanical loading influences osteocyte-derived exosome secretion through calcium influx and interplay within the CAMKII/CREB pathway.

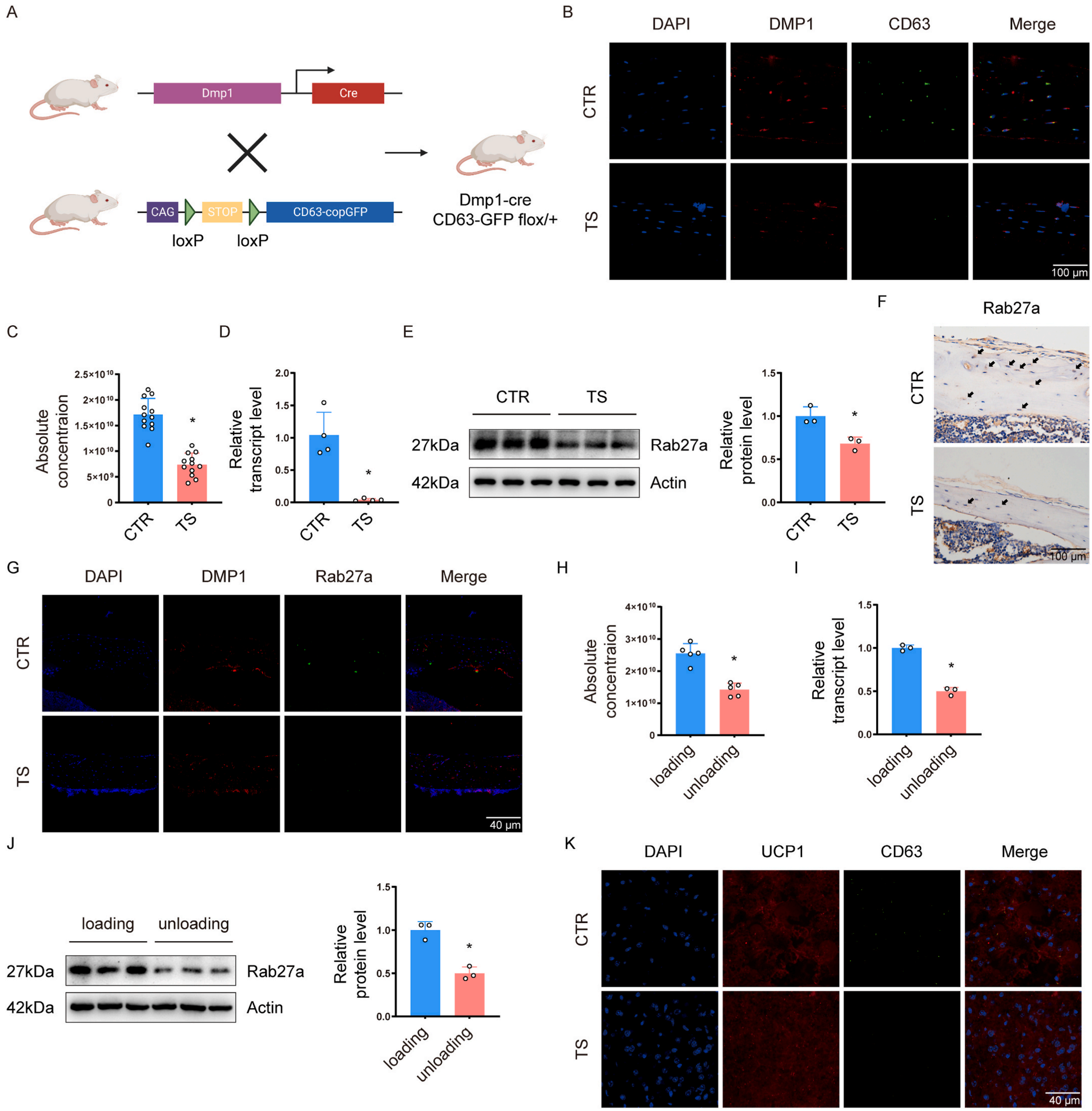

Fig. 2. The secretion of exosomes derived from osteocytes was decreased due to mechanical unloading. (A) A diagram illustrating the construction of osteocyte-specific CD63 reporter mice. (B) Representative images of CD63-positive osteocytes in bone tissue from both CTR and TS group. Nuclei are stained in blue with DAPI, while osteocytes are labeled using DMP1. (C) Absolute concentration of exosomes secreted by ex vivo bone tissue. (D) Transcript level, (E) WB analysis and relevant quantification analysis of Rab27a in bone tissue. Representative images of Rab27a-positive osteocytes in bone tissue.(F) Arrows indicating positive cells, and (G) osteocytes are labeled using DMP1. (H) Absolute concentration of exosomes secreted by osteocytes from both loading and unloading group. (I) Transcript level, (J) WB analysis and relevant quantification analysis of Rab27a in osteocytes. (K) Representative images of osteocyte-specific exosomes in BAT from both CTR and TS group. Osteocyte-specific exosomes are CD63-positive. All data are Mean ± SD. *P < 0.05. (For interpretation of the references to color in this figure legend, the reader is referred to the Web version of this article.)

3.4. *Osteocyte exosomes regulate thermogenic activity of brown adipocytes*

Previously, our findings demonstrated that mechanical loading exerts an impact on the secretion of osteocyte-derived exosomes. To investigate the impact of osteocyte exosomes on the thermogenic activity of brown adipocytes, bone tissues were isolated and cultured (Fig. 4A). The supernatant was collected to extract equal amounts of exosomes for primary brown adipocytes or local injection into BAT. We observed an upregulation in the transcriptional level of *Ucp1* and increased protein expression levels of UCP1 and PGC1α in TS exosome-treated brown adipocytes (Fig. 4B and C), indicating enhanced

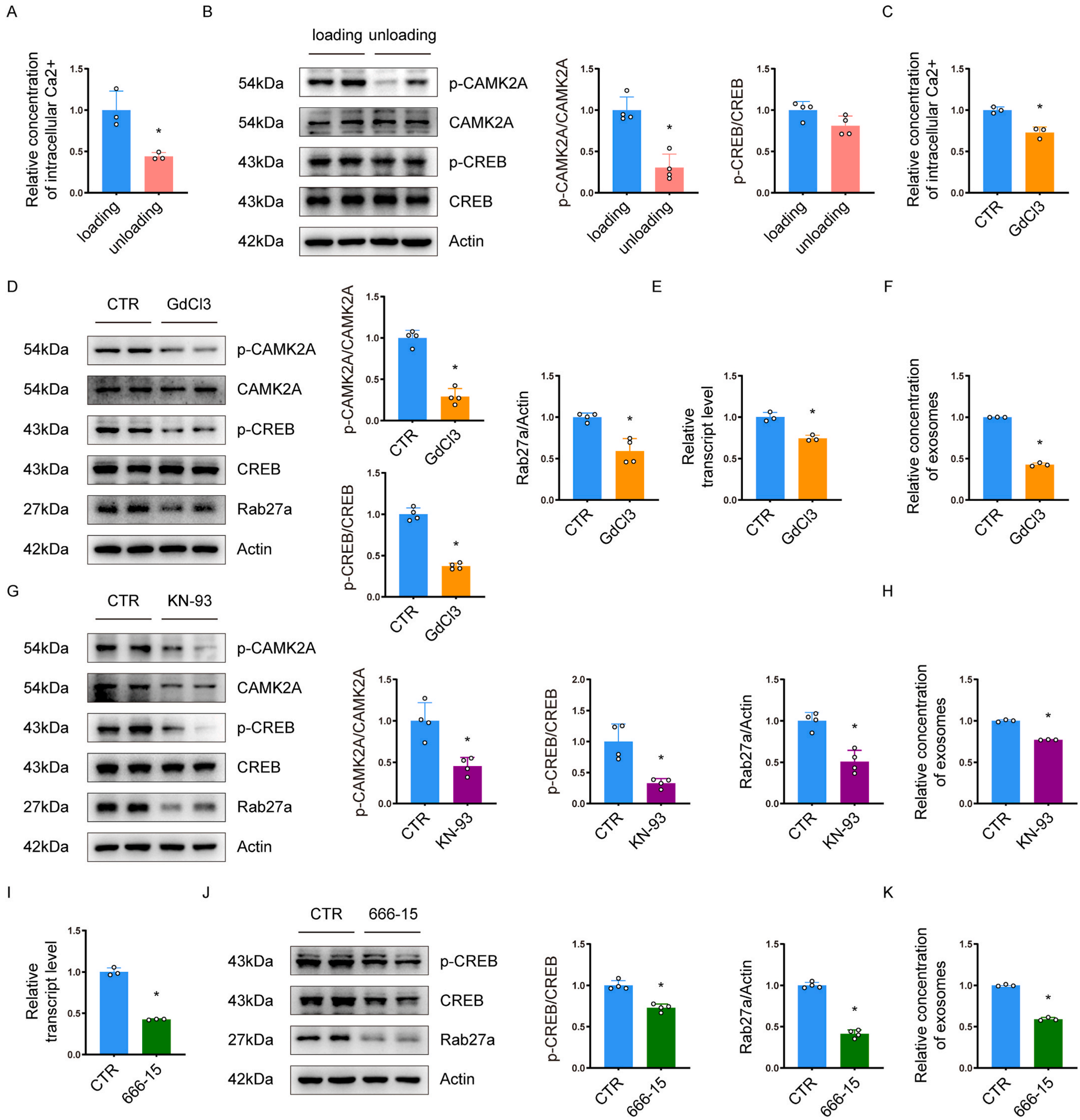

Fig. 3. The exosome secretion of osteocytes is modulated by mechanical loading via the CAMKII/CREB signaling pathway. The osteocytes were either exposed to mechanical loading (loading group) or not (unloading group). (A, B) (A) Intracellular calcium level was measured; (B) WB analysis and quantification analysis were performed. The osteocytes were either treated with GdCl3 (GdCl3 group) or not (CTR group), while exposed to mechanical loading. (C) Intracellular calcium level; (D) WB analysis and relevant quantification analysis; (E) Transcript level of Rab27a; (F) Relative concentration of exosomes secreted by osteocytes. The osteocytes were either treated with KN-93 (KN-93 group) or not (CTR group), while exposed to mechanical loading. (G, H) (G) WB analysis and relevant quantification analysis; (H) Relative concentration of exosomes secreted by osteocytes. The osteocytes were either treated with 666-15 (666-15 group) or not (CTR group), while exposed to mechanical loading. (I–K) (I) Transcript level of Rab27a; (J) WB analysis and relevant quantification analysis; (K) Relative concentrations of exosomes secreted by osteocytes. All data are Mean ± SD. $^{*}P < 0.05$.

thermogenic activity. Additionally, images of H&E staining revealed smaller lipid vacuoles and denser tissue structure within BAT of TS-exo group (Fig. 4D). Furthermore, we found higher expression levels of thermogenesis-related proteins in the TS-exo group (Fig. 4E). Interestingly, no significant change in BAT thermogenic activity was observed when treated with TS exosomes compared to PBS treatment, suggesting that loading-induced osteocyte exosomes inhibit BAT thermogenic activity while unloaded osteocyte exosomes restore it to its previous state. Based on this observation, we hypothesized that similar to their effect on the number of osteocyte-derived exosomes, loading may induce an

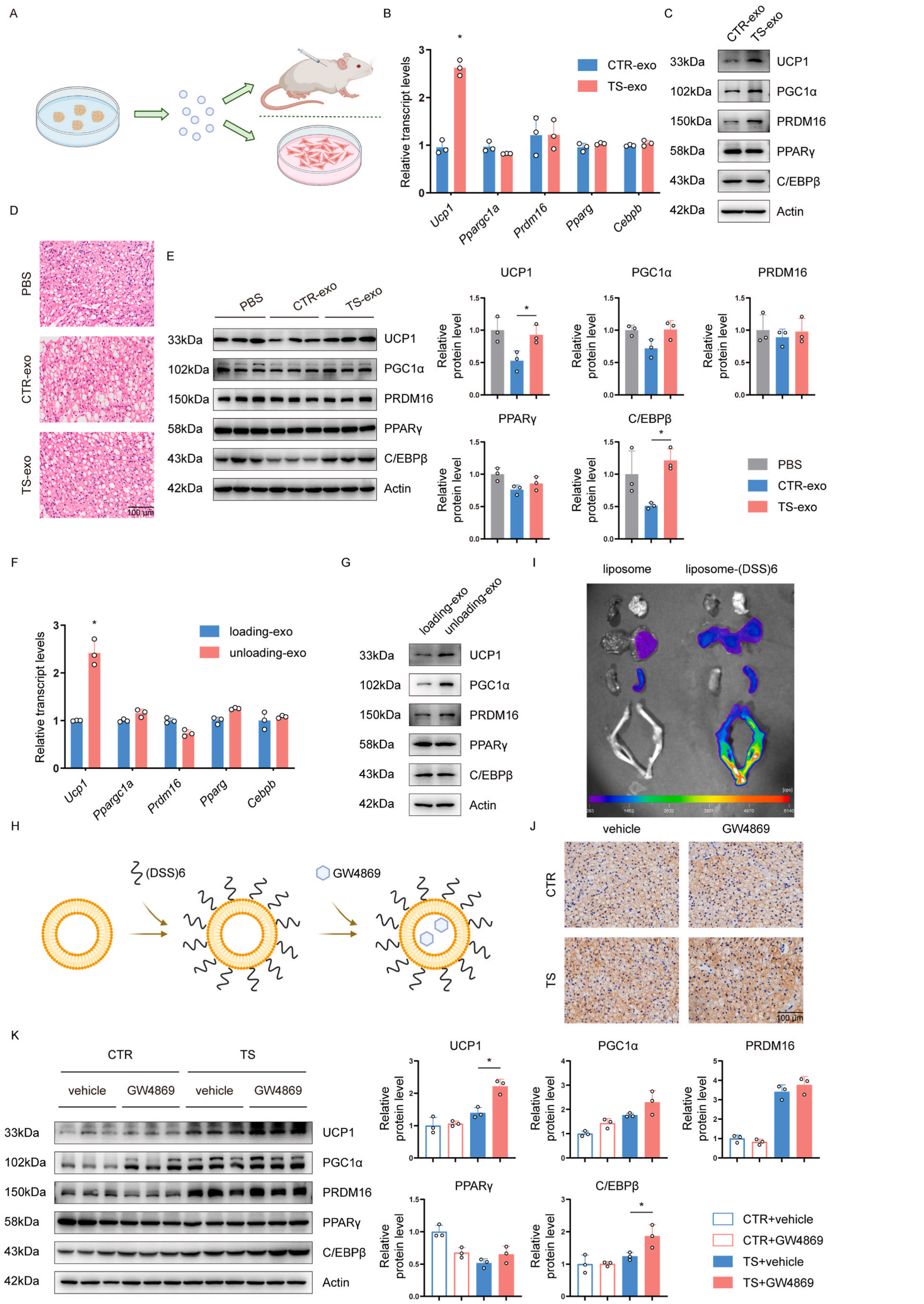

(caption on next page)

Fig. 4. The exosomes released by osteocytes under mechanical unloading conditions resulted in an augmentation of thermogenic activity in brown adipocytes. (A) A diagram depicts that the exosomes were extracted from bone tissue and followed by local injection or treatment of cells. (B) Transcript levels of thermogenic genes, (C) WB analysis of thermogenic proteins in primary brown adipocytes treated with bone-derived exosomes. (D) Representative H&E staining images of BAT; (E) WB analysis and relevant quantitative analysis of thermogenic proteins of BAT after local injection of exosomes derived from bone tissue. (F) Transcript levels of thermogenic genes, and (G) WB analysis of thermogenic proteins in primary brown adipocytes treated with exosomes stimulated by mechanical loading in vitro. (H) A diagram illustrating the construction of bone-targeted liposomes. (I) Fluorescence imaging showed that liposomes with target heads targeted bone tissue. Mice were injected with or without bone-targeted GW4869 via tail vein while exposed to mechanical loading. (J, K) (J) Representative images of IHC staining of BAT; (K) WB analysis and quantification analysis of thermogenic proteins in BAT. All data are Mean ± SD. *P < 0.05. (For interpretation of the references to color in this figure legend, the reader is referred to the Web version of this article.)

increase in certain substances within exosomes which subsequently inhibits BAT's thermogenic activity, while unloading restores the previous state. Subsequently, primary brown adipocytes were treated with mechanically stimulated exosomes derived from osteocytes exposed in vitro. In line with the in vivo loading effect, exosomes derived from the mechanical loading group were observed to suppress the thermogenic activity of brown adipocytes (Fig. 4F and G). Additionally, the supernatant in which exosomes were removed had no modulatory effect on brown adipocytes (Figs. S3A and S3B), proving our conjecture from a different perspective.

In order to further investigate the regulatory effect of osteocyte exosomes on BAT in vivo, we developed a GW4869@DSPE-PEG$_{2000}$-MAL-(DSS)$_6$ conjugate to selectively reduce the osteocyte-derived exosomes in vivo (Fig. 4H). DSS6 specifically targets bone tissue (Fig. 4I) while GW4869 inhibits exosome secretion. Subsequently, mice were subjected to tail vein injections of liposomes with or without GW4869 for a duration of 4 weeks under both loading and unloading conditions. The liposomes were found to be no harm to organs (Fig. S3C). Our results revealed that UCP1 expression was elevated in the TS-vehicle group compared to the CTR-vehicle group, and this elevation was further enhanced in the TS-GW4869 group (Fig. 4J and K). Similarly, protein expression levels of PGC1α and CEBPβ were higher in the TS-GW4869 group than those observed in the TS-vehicle group (Fig. 4K), indicating that reduction of osteocyte-secreted exosomes during mechanical unloading could potentiate BAT thermogenic activity. Taken together with our previous findings, it was revealed that exosomes secreted by osteocytes under mechanical loading exerted inhibitory effects on BAT thermogenic activity. Furthermore, during mechanical unloading, a reduction in exosome secretion from osteocytes weakened their inhibitory effect on thermogenic activity and consequently enhanced BAT's thermogenic capacity.

3.5. Let-7e-5p contained in osteocyte exosomes inhibited the thermogenic activity of brown adipocytes

To investigate the content of osteocyte exosomes that regulate the thermogenic activity of brown adipocytes, considering their abundance in miRNAs, we generated DMP1-specific Dicer knockout mice to achieve osteocyte-targeted knockdown of miRNAs in vivo (Fig. 5A). We isolated circulating exosomes from DMP1-cre; Dicerfl/fl mice and Dicerfl/fl mice for miRNA sequencing analysis, identifying significantly downregulated miRNAs in Dicer-cKO mice as potential osteocyte-secreted exosome miRNAs (Fig. 5B). Additionally, we re-analyzed the data of differential miRNA expression in osteocytes under mechanical stress from the GEO public database (GSE179199). 163 miRNAs were upregulated while 65 were downregulated (Fig. 5C). Combining these findings with our previous results, we selected 163 upregulated miRNAs and osteocyte-derived exosome miRNAs for co-analysis and identified let-7e-5p as an osteocyte-specific exosome miRNA positively regulated by mechanical stress (Fig. 5D). Furthermore, during the differentiation of primary brown adipocytes, we observed a concurrent decrease in let-7e-5p expression alongside increased *Ucp1* expression (Fig. 5E), indicating a negative correlation between let-7e-5p and Browning. Consistent with our hypothesis, let-7e-5p expression was reduced in bone tissue (Fig. 5F), osteocyte-derived exosomes (Fig. 5G), circulating exosomes (Fig. 5H), and BAT (Fig. 5I) of TS group. Similarly, we found that let-7e-5p is decreased in osteocytes treated with mechanical unloading (Fig. 5J). However, it is worth noting that the reduction of let-7e-5p levels may not solely be attributed to decreased secretion by osteocytes but could also involve reduced production by BAT itself. To elucidate the underlying cause, further investigation was conducted on pri-let-7e expression level (Fig. 5K and L), revealing a decrease specifically only within bone after mechanical unloading. Therefore, the expression of let-7e-5p in BAT was influenced by osteocytes. These findings provide evidence suggesting that let-7e-5p is a loading-responsive miRNA derived from osteocytes, which can regulate the thermogenic activity of BAT via circulating exosomes.

The role of Let-7e-5p in the regulation of thermogenic activity of brown adipocytes necessitates further investigation. Following transfection of let-7e-5p mimic into primary brown adipocytes, there was observed downregulation in the transcript levels of *Ucp1*, *Ppargc1a* and other thermogenic genes (Fig. 5M), accompanied by a decrease in the expression levels of corresponding thermogenic proteins (Fig. 5N). Conversely, transfection with let-7e-5p inhibitor resulted in an increase in markers associated with thermogenesis (Fig. 5O and P). These findings collectively indicate that let-7e-5p inhibits differentiation and suppresses thermogenic activity of primary brown adipocytes.

3.6. Let-7e-5p modulates the thermogenic activity of brown adipocytes by targeting Ppargc1a

In order to investigate the targeted mRNA of let-7e-5p, we conducted a comprehensive screening of let-7e-5p target genes using miRNA target prediction tools (TargetScan, miRmap, miRDB) (Fig. 6A). A total of 588 candidate genes were identified through this analysis. Additionally, we retrieved transcriptome data from the GEO database (GSE200650) for BAT exposed to low temperature and performed re-analysis. This analysis revealed differentially expressed genes in BAT under low temperature conditions (Fig. 6B). The volcano plot displayed an upregulation of 249 genes in the low temperature environment (Fig. 6C), suggesting their potential involvement in thermogenesis. We further analyzed these 249 thermogenic-related genes along with the previously identified 588 candidate target genes and *Ppargc1a* was discovered (Fig. 6D). Dual luciferase assay were designed (Fig. 6E) and confirmed that let-7e-5p directly targets *Ppargc1a* as predicted by our bioinformatics analysis (Fig. 6F). To further validate our findings, we locally injected AAV encapsulated let-7e-5p into BAT and observed down-regulation of *Ppargc1a* expression as well as other thermogenic-related genes in the control group (Fig. 6G). The expression levels of proteins related to thermogenesis were also found to be down-regulated (Fig. 6H). Local administration of AAV-let-7e-5p effectively reversed the unloading-induced up-regulation thermogenic markers in the TS group. The functional role of AAV-let-7e-5p was further confirmed through IHC staining of UCP1 (Fig. 6I). In summary, our findings demonstrate that let-7e-5p targets *Ppargc1a* to modulate thermogenic activity in brown adipocytes, and the detrimental effects of mechanical unloading on BAT can be counteracted by localized injection of AAV-let-7e-5p.

4. Discussion

In this study, we have identified exosomes as an intermediary link in the remote regulation of BAT by osteocytes. Our findings suggest that

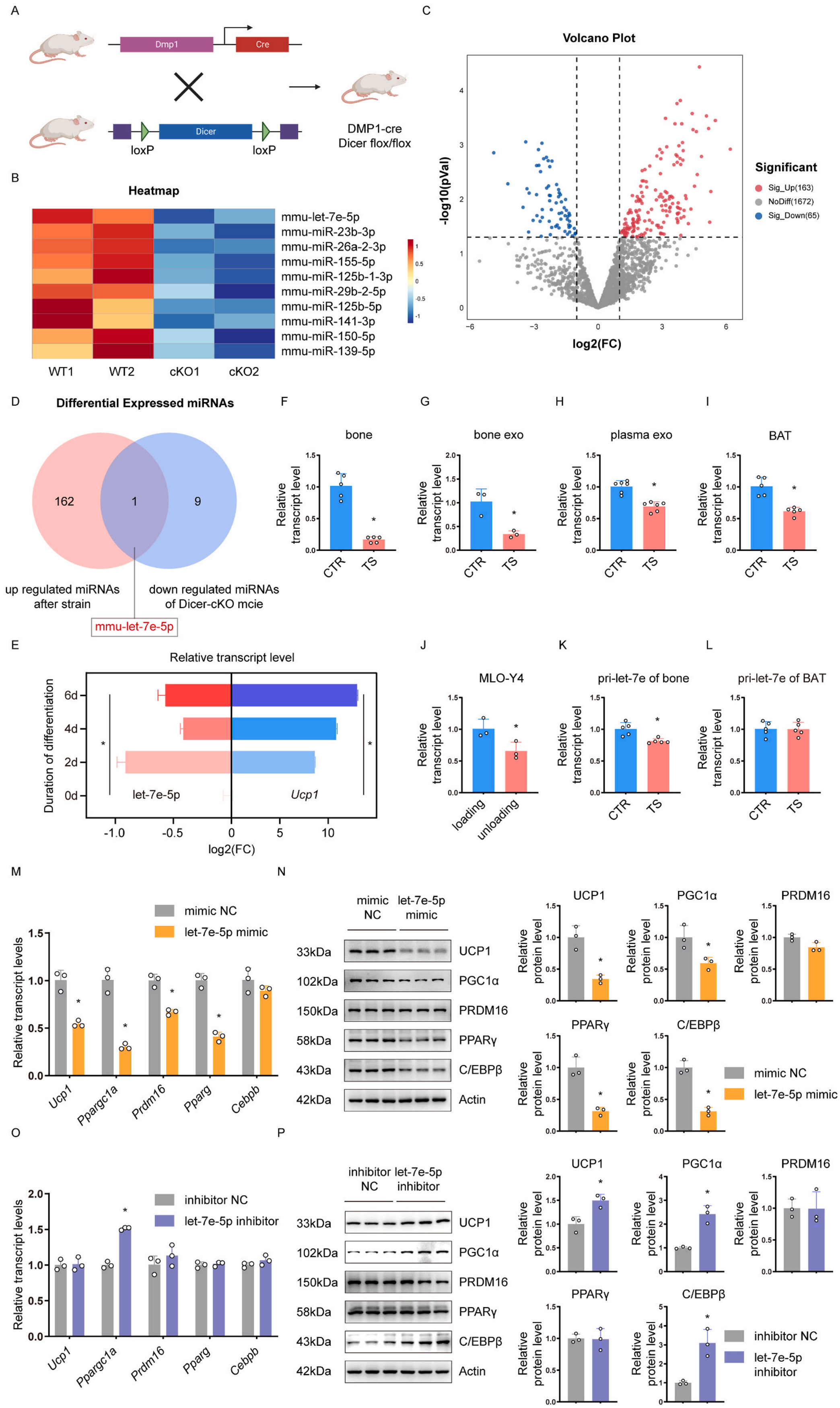

(caption on next page)

Fig. 5. Let-7e-5p inhibits thermogenic activity in brown adipocytes. (A) A diagram illustrating the construction of osteocyte-specific Dicer knockout mice. (B) Heatmap of miRNAs in circulating exosomes derived from osteocytes. (C) Volcano plot of miRNAs stimulated by mechanical strain in osteocytes. (D) The Venn diagram illustrates the miRNAs that are simultaneously downregulated in B and upregulated in C. (E) Transcriptional alterations of let-7e-5p and *Ucp1* throughout the process of brown adipocyte differentiation. Transcript level of let-7e-5p in (F) bone tissue, (G) bone-derived exosomes, (H) circulating exosomes, (I) BAT from TS group and CTR group, and (J) osteocytes from loading group and unloading group. Transcript level of pri-let-7e in (K) bone tissue, and (L) BAT from TS group and CTR group. (M) Transcript levels of thermogenic genes in primary brown adipocytes transfected with mimic control or let-7e-5p mimic. (N) WB analysis and relevant quantitative analysis of thermogenic proteins in primary brown adipocytes transfected with mimic control or let-7e-5p mimic. (O) Transcript levels of thermogenic genes in primary brown adipocytes transfected with inhibitor control or let-7e-5p inhibitor. (P) WB analysis and relevant quantitative analysis of thermogenic proteins in primary brown adipocytes transfected with inhibitor control or let-7e-5p inhibitor. All data are Mean ± SD. *P < 0.05. (For interpretation of the references to color in this figure legend, the reader is referred to the Web version of this article.)

mechanical loading enhances exosome secretion in osteocytes through the calcium signaling pathway, and influences the production and release of let-7e-5p in osteocytes. Furthermore, these exosomes encapsulate let-7e-5p and regulate the thermogenic activity of BAT.

Our study revealed an increase in BAT thermogenic activity under conditions of skeletal unloading. The increased thermogenesis in the BAT will break the balance of body temperature, and will disturb normal physiological activities. The induced consequence is difficult to deal with in some cases, especially for the astronauts suffering from the mechanical unloading at the space. Astronauts were observed to experience a gradual and continuous increase in the resting core body temperature, amounting to approximately 1 °C over a span of 2.5 months [36,37], implying the potential existence of long-term physiological adaptations. Additionally, researchers observed modifications in BAT thermogenic activity during space flight, which are closely associated with maintaining body temperature stability [18]. These phenomena can be well explained by our findings. Our investigation demonstrated higher core body temperatures after prolonged cold exposure in mice of TS group compared to CTR group, indicating enhanced cold resistance due to mechanical unloading. This supports the notion that increased core body temperature observed among astronauts may be related to microgravity. Moreover, we discovered that mechanical unloading induces changes in BAT thermogenic activity suggesting its potential association with microgravity-induced alterations in space. Collectively, these analyses suggest that microgravity affects BAT thermogenic activity thereby influencing core body temperature regulation. However, it is important to acknowledge limitations within this explanation. Firstly, microgravity may not be the sole factor impacting astronaut's core body temperature while the tail suspension model only partially simulates microgravity effects experienced by astronauts. Researchers have found that the space environment may induce heightened sympathetic tone in astronauts [38], subsequently leading to an elevation in body temperature. Furthermore, the absence of gravity in space hampers effective air convection, which can also impact body temperature regulation [39]. However, considering the gradual increase in core body temperature over a prolonged period of 2.5 months among astronauts, these explanations may not hold true. This is because both factors - increased sympathetic tone and impaired air convection - are expected to manifest immediately upon entering space and result in a rapid rise in body temperature, contradicting the observed phenomenon. In addition, short-term effects caused by mechanical unloading were also examined in the study (Fig. S4A). We found that one week of treatment was not sufficient to cause significant changes, so the effects of unloading should be considered as long-term effects. The second limitation is that body temperature stability is not only associated with BAT, but also with the hypothalamus, metabolism, and other factors [38]. In this study, we focused solely on BAT as a representative thermogenic tissue; however, further investigation is required to explore the influence of other factors. Additionally, while we selected osteocytes as the key point for our study, it is also important to consider exploring mechanical unloading of muscle.

Osteocytes have long been recognized as being regulated by mechanical loading. Previous studies have demonstrated that osteocytes undergo not only morphological changes but also alterations in substance secretion following stress stimulation [40]. For instance, it has been observed that circulating sclerostin level increase in both humans and animal models during prolonged bed rest or immobilization [41–43], conditions characterized by a lack of mechanical loading on osteocytes. Consistent with this, the secretion of sclerostin by osteocytes was found to be strongly associated with mechanical loading. The findings revealed that a decrease in loading results in an increase in the secretion of sclerostin, whereas loading stimulation inhibits its release [44,45]. Similarly, researchers found that mechanical loading could stimulate the secretion of extracellular vesicles from osteocytes [46]. In our present study, we discovered for the first time that exosome secretion is influenced by mechanical loading in osteocytes. We observed decreased exosome secretion and reduced expression of Rab27a, a critical regulator of exosome release, under conditions of mechanical unloading using both a mouse tail suspension model and an in vitro cellular stress model. Based on the crucial role played by Rab27a in exosome secretion, we speculated that mechanical stress may impact exosome release through modulation of Rab27a expression level. Notably, the phenomenon of enhanced exosome production in response to mechanical loading is not exclusive to osteocytes. Similar findings were reported when investigating the effect of mechanical tension on exosomes derived from C2C12 cells [47]. Furthermore, these mechanically induced exosomes exhibited altered biological functions along with modifications in their miRNA content, which aligns well with our observations.

Further investigation is warranted to elucidate the regulatory role of mechanical loading on exosome secretion by osteocytes. Previous studies have demonstrated that loaded osteocytes can induce various signaling changes, including calcium, ATP, nitric oxide, prostaglandin, etc [48]. Among these, the calcium signaling pathway primarily mediates intracellular signal transduction. In vivo application of calcium channel inhibitors has been shown to reduce bone response to mechanical loading, while pharmacological inhibition of calcium channels impairs osteocyte's ability to respond to mechanical signals, suggesting a crucial role for calcium in regulating loaded osteocytes [48]. Consistently, we observed that inhibiting calcium influx with Gd attenuated the increased exosome secretion induced by loading, highlighting the significance of calcium signaling in loading-induced exosome secretion. Additionally, we investigated downstream signaling pathways potentially triggered by calcium influx. CAMKII/CREB is an important downstream calcium influx pathway [22], and CREB acts as a transcription factor for Rab27a expression [34,35]. By assessing phosphorylation levels of CAMKII and CREB and employing specific inhibitors for both proteins, we confirmed their involvement in mediating Rab27a expression induced by calcium influx. However, it should be noted that besides the calcium signaling pathway discussed above, other potential signal transduction pathways may also play a role in loaded osteocytes and warrant further investigation.

The targeted delivery system is a promising field for the treatment of various diseases. Previous study has shown that $(DSS)_6$ has a high affinity for hydroxyapatite and calcium phosphate on bone surface [30]. In this study, we used a liposome with the $(DSS)_6$ target to deliver GW4869 to bone tissue, which confirmed that the exosomes secreted by osteocytes regulate BAT remotely. The use of liposomes targeting osteocytes can regulate the physiological and pathological processes of osteocytes, thereby regulating the homeostasis of the body.

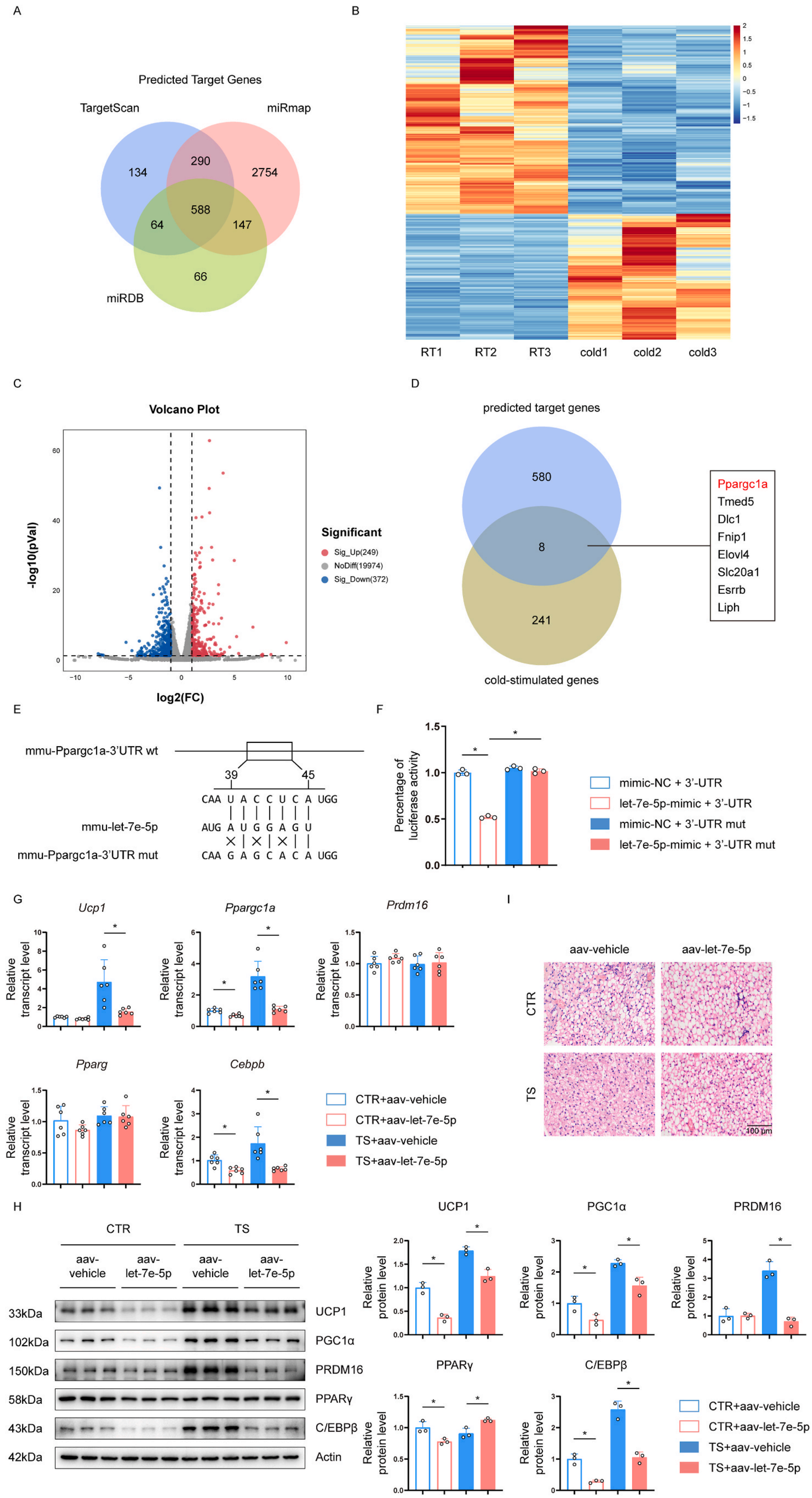

(caption on next page)

Fig. 6. Let-7e-5p regulates thermogenic activity in brown adipocytes by targeting *Ppargc1a*. (A) Predicted genes targeted by let-7e-5p. (B) Heatmap of the differential expressed genes regulated by low temperature environment. (C) Volcano plot of the differential expressed genes induced by low temperature environment. (D) The genes both upregulated by low temperature environment and targeted by let-7e-5p. Dual-luciferase assay was designed (E) and showed that let-7e-5p targets *Ppargc1a* (F). Mice were locally injected with aav-control or aav-let-7e-5p while exposed to mechanical loading. (G–I) (G) Transcript levels of thermogenic genes; (H) WB analysis and relevant quantitative analysis of thermogenic proteins; (I) Representative images of H&E staining were provided. All data are Mean ± SD. *P < 0.05. (For interpretation of the references to color in this figure legend, the reader is referred to the Web version of this article.)

In recent years, the involvement of osteocyte exosomes in various physiological and pathological processes has been discovered [7,10,49]. In this study, we found that osteocyte exosomes play a role in regulating the thermogenic activity of BAT, and the expression levels of exosome-encapsulated miRNAs were modulated under mechanical loading. Previous studies have identified changes in circulating exosome miRNAs following osteocyte-specific ablation to screen for osteocyte-specific miRNAs [8]. However, systemic ablation of osteocytes significantly impacts overall body homeostasis and may introduce confounding factors from other tissues or organs that interfere with exosome release and content composition. To address these limitations, we generated mice with osteocyte-specific Dicer knockout to achieve targeted knockdown of miRNA within osteocyte-derived exosomes for identification purposes. Compared to previous approaches, our method offers improved specificity and accuracy. Furthermore, we analyzed the miRNA dataset obtained from loaded osteocytes. To avoid data clutter caused by widespread effects on multiple tissues or organs, sequencing and analysis of circulating exosome miRNAs were not performed. The validation of let-7e-5p was confirmed in both circulating exosomes and osteocyte exosomes, while the levels of pri-let-7e were further examined in bone tissue and BAT to elucidate the underlying cause for the observed alterations in let-7e-5p.

Although we have preliminarily explained the effect of bone on BAT, the effect of BAT on bone still needs to be explored. As a strong stimulus, cold exposure was found to negatively affect bone remodeling in 2013 for the first time [50]. However, impaired BAT function leads to bone loss [50], indicating that BAT may be a protective factor. Further research showed that UCP1 may play a vital role in the interaction. UCP1(−/−) mice housed at 22 °C showed significantly lower cancellous bone mass, with lower trabecular number and thickness, compared to wild type mice housed at the same temperature [51]. Importantly, these altered bone phenotypes were not observed when UCP1(−/−) and wild type mice were housed in thermo-neutral conditions, indicating a UCP1 dependent support of bone mass and bone formation at the lower temperature [51]. These results suggest that increased BAT activity may alleviate bone loss to some extent under adverse conditions such as cold stimulation and mechanical unloading, while impaired BAT activity may aggravate bone loss. The effects of BAT on bone deserve further study to perfect the crosstalk between bone and BAT.

In summary, we have identified a previously unknown mechanism that underlies the enhanced thermogenic activity of BAT during mechanical unloading conditions. Distinct loading states modulate the secretion of osteocyte-derived exosomes and their cargo, thereby remotely regulating thermogenic activity of BAT. Targeting this mechanism by manipulating exosome release from osteocytes holds promise for maintaining overall body homeostasis and may also have potential applications in regulating body temperature among astronauts.

Author contributions

All authors contributed to the study. The first draft of the manuscript was written by Yuze Ma and all authors commented on previous versions of the manuscript. All authors read and approved the final manuscript.

Data availability

The datasets generated during and/or analysed during the current study are not publicly available due to unpublished further research but are available from the corresponding author on reasonable request.

Ethics approval

This study was performed in line with the principles of the Declaration of Helsinki. Approval was granted by the Ethics Committee of Nanjing Drum Tower Hospital.

Consent for publication

Not applicable.

Declaration of competing interest

The authors declare that they have no known competing financial interests or personal relationships that could have appeared to influence the work reported in this paper.

Acknowledgements

This work was supported by the National Key Research and Development Project (2021YFA1201404), Major Project of NSFC (81991514), Jiangsu Province Medical Innovation Center of Orthopedic Surgery (CXZX202214), Jiangsu Provincial Key Medical Center Foundation, Jiangsu Provincial Medical Outstanding Talent Foundation, Jiangsu Provincial Medical Youth Talent Foundation and Jiangsu Provincial Key Medical Talent Foundation, the Fundamental Research Funds for the Central Universities (14380493, 14380494).

Appendix A. Supplementary data

Supplementary data to this article can be found online at https://doi.org/10.1016/j.jot.2024.06.012.

References

[1] Su N, Yang J, Xie Y, Du X, Chen H, Zhou H, et al. Bone function, dysfunction and its role in diseases including critical illness. Int J Biol Sci 2019;15(4):776–87. https://doi.org/10.7150/ijbs.27063.

[2] Han Y, You X, Xing W, Zhang Z, Zou W. Paracrine and endocrine actions of bone - the functions of secretory proteins from osteoblasts, osteocytes, and osteoclasts. Bone Research 2018;6(1):1–11. https://doi.org/10.1038/s41413-018-0019-6.

[3] Robling AG, Bonewald LF. The osteocyte: new insights. Annu Rev Physiol 2020;82: 485–506. https://doi.org/10.1146/annurev-physiol-021119-034332.

[4] Geoghegan IP, Hoey DA, McNamara LM. Integrins in osteocyte biology and mechanotransduction. Curr Osteoporos Rep 2019:195–206. https://doi.org/10.1007/s11914-019-00520-2.

[5] Oh H, Park SY, Cho W, Abd El-Aty AM, Hacimuftuoglu A, Kwon CH, et al. Sclerostin aggravates insulin signaling in skeletal muscle and hepatic steatosis via upregulation of ER stress by mTOR-mediated inhibition of autophagy under hyperlipidemic conditions. J Cell Physiol 2022;237(11):4226–37. https://doi.org/10.1002/jcp.30873.

[6] Li W, Zhang Y, Su Y, Hao Y, Wang X, Yin X, et al. Intracerebroventricular injection of sclerostin reduced social hierarchy and impaired neuronal dendritic complexity in mice. Neurosci Lett 2022;773:136514. https://doi.org/10.1016/j.neulet.2022.136514.

[7] Lv PYP, Gao PFF, Tian GGJ, Yang Y-YYY, Mo F-FFF, Wang Z-HZH, et al. Osteocyte-derived exosomes induced by mechanical strain promote human periodontal ligament stem cell proliferation and osteogenic differentiation via the miR-181b-5p/PTEN/AKT signaling pathway. 295-Article No.: 295 Stem Cell Res Ther 2020; 11(1). https://doi.org/10.1186/s13287-020-01815-3.

[8] Sato M, Suzuki T, Kawano M, Tamura M. Circulating osteocyte-derived exosomes contain miRNAs which are enriched in exosomes from MLO-Y4 cells. Biomedical Reports 2017;6(2):223–31. https://doi.org/10.3892/br.2016.824.

[9] Mathivanan S, Ji H, Simpson RJ. Exosomes: extracellular organelles important in intercellular communication. J Proteonomics 2010;73(10):1907–20. https://doi.org/10.1016/j.jprot.2010.06.006.
[10] Cheng F, Wang Z, You G, Liu Y, He J, Yang J. Osteocyte-derived exosomes confer multiple myeloma resistance to chemotherapy through acquisition of cancer stem cell-like features. Leukemia 2023;37(6):1392–6. https://doi.org/10.1038/s41375-023-01896-y.
[11] Scheele C, Wolfrum C. Brown adipose crosstalk in tissue plasticity and human metabolism. Endocr Rev 2020;41(1):53–65. https://doi.org/10.1210/endrev/bnz007.
[12] Kong X, Yao T, Zhou P, Kazak L, Tenen D, Lyubetskaya A, et al. Brown adipose tissue controls skeletal muscle function via the secretion of myostatin. Cell Metabol 2018;28(4):631–643.e3. https://doi.org/10.1016/j.cmet.2018.07.004.
[13] Stanford KI, Lynes MD, Takahashi H, Baer LA, Arts PJ, May FJ, et al. 12,13-diHOME: an exercise-induced lipokine that increases skeletal muscle fatty acid uptake. Cell Metabol 2018;27(5):1111–1120.e3. https://doi.org/10.1016/j.cmet.2018.03.020.
[14] Zheng Y, He J, Yang D, Yuan M, Liu S, Dai F, et al. Irisin reduces the abnormal reproductive and metabolic phenotypes of PCOS by regulating the activity of brown adipose tissue in mice. Biol Reprod 2022;107(4):1046–58. https://doi.org/10.1093/biolre/ioac125.
[15] Liu C, Liu J, Wang T, Su Y, Li L, Lan M, et al. Immunoglobulin superfamily containing leucine-rich repeat (islr) participates in IL-6-mediated crosstalk between muscle and Brown adipose tissue to regulate energy homeostasis. Int J Mol Sci 2022;23(17). https://doi.org/10.3390/ijms231710008.
[16] Du J, He Z, Xu M, Qu X, Cui J, Zhang S, et al. Brown adipose tissue Rescues bone loss induced by cold exposure. Front Endocrinol 2022;12(January):1–10. https://doi.org/10.3389/fendo.2021.778019.
[17] Lidell ME, Enerbäck S. Brown adipose tissue and bone. Int J Obes Suppl 2015;5 (S1):S23–7. https://doi.org/10.1038/ijosup.2015.7.
[18] Wong CP, Iwaniec UT, Turner RT. Evidence for increased thermogenesis in female C57BL/6J mice housed aboard the international space station. Npj Microgravity 2021;7(1). https://doi.org/10.1038/s41526-021-00150-y.
[19] Yamashita H, Ohira Y, Wakatsuki T, Yamamoto M, Kizaki T, Oh-Ishi S, et al. Responses of brown adipose tissue activity to unloading in rats. J Appl Physiol 1995;78(2):384–7. https://doi.org/10.1152/jappl.1995.78.2.384.
[20] Sun W, Chi S, Li Y, Ling S, Tan Y, Xu Y, et al. The mechanosensitive Piezo1 channel is required for bone formation. Elife 2019;8. https://doi.org/10.7554/eLife.47454.
[21] Murthy SE, Dubin AE, Whitwam T, Jojoa-cruz S, Cahalan SM, Ali S, et al. OSCA/TMEM63 are an evolutionarily conserved family of mechanically activated ion channels. Elife 2018:1–17.
[22] Wong MH, Samal AB, Lee M, Vlach J, Novikov N, Niedziela-Majka A, et al. The KN-93 molecule inhibits calcium/calmodulin-dependent protein kinase II (CaMKII) activity by binding to Ca(2+)/CaM. J Mol Biol 2019;431(7):1440–59. https://doi.org/10.1016/j.jmb.2019.02.001.
[23] Yan J, Xu W, Lenahan C, Huang L, Wen J, Li G, et al. CCR5 activation promotes NLRP1-dependent neuronal pyroptosis via CCR5/PKA/CREB pathway after intracerebral hemorrhage. Stroke 2021;52(12):4021–32. https://doi.org/10.1161/STROKEAHA.120.033285.
[24] Shah KM, Stern MM, Stern AR, Pathak JL, Bravenboer N, Bakker AD. Osteocyte isolation and culture methods. BoneKEy Rep 2016;5. https://doi.org/10.1038/BONEKEY.2016.65.
[25] Gooi JH, Chia LY, Vrahnas C, Sims NA. Isolation, purification, generation, and culture of osteocytes. Methods Mol Biol 2019;1914:39–51. https://doi.org/10.1007/978-1-4939-8997-3_3.
[26] Gantner ML, Hazen BC, Conkright J, Kralli A. GADD45γ regulates the thermogenic capacity of brown adipose tissue. Proc Natl Acad Sci USA 2014;111(32):11870–5. https://doi.org/10.1073/pnas.1406638111.
[27] Gao, W., Kong, X., Yang, Q., n.d. Isolation, primary culture, and differentiation of preadipocytes from mouse Brown adipose tissue vol. 1566: 3–8, Doi: 10.1007/978-1-4939-6820-6..
[28] Chouchani ET, Kazak L, Jedrychowski MP, Lu GZ, Erickson BK, Szpyt J, et al. Mitochondrial ROS regulate thermogenic energy expenditure and sulfenylation of UCP1. Nature 2016;532(7597):112–6. https://doi.org/10.1038/nature17399.
[29] Yang D, Zhang W, Zhang H, Zhang F, Chen L, Ma L, et al. Progress, opportunity, and perspective on exosome isolation - efforts for efficient exosome-based theranostics. Theranostics 2020;10(8):3684–707. https://doi.org/10.7150/thno.41580.
[30] Liang C, Peng S, Li J, Lu J, Guan D, Jiang F, et al. Inhibition of osteoblastic Smurf1 promotes bone formation in mouse models of distinctive age-related osteoporosis. Nat Commun 2018;9(1):3428. https://doi.org/10.1038/s41467-018-05974-z.
[31] Ostrowski M, Carmo NB, Krumeich S, Fanget I, Goud B, Benaroch P, et al. Rab27a and Rab27b control different steps of the exosome secretion pathway. Nat Cell Biol 2010;12(1):19–30.
[32] Lv Z, Xu X, Sun Z, Yang YX, Guo H, Li J, et al. TRPV1 alleviates osteoarthritis by inhibiting M1 macrophage polarization via Ca2+/CaMKII/Nrf2 signaling pathway. Cell Death Dis 2021;12(6). https://doi.org/10.1038/s41419-021-03792-8.
[33] Rolewska P, Simm A, Silber RE, Bartling B. Reduced expression level of the cyclic adenosine Monophosphate response element-binding protein contributes to lung aging. Am J Respir Cell Mol Biol 2014;50(1):201–11. https://doi.org/10.1165/rcmb.2013-0057OC.
[34] An X, Lv J, Wang F. Pterostilbene inhibits melanogenesis, melanocyte dendricity and melanosome transport through cAMP/PKA/CREB pathway. Eur J Pharmacol 2022;932(August):175231. https://doi.org/10.1016/j.ejphar.2022.175231.
[35] Noguchi S, Kumazaki M, Mori T, Baba K, Okuda M, Mizuno T, et al. Analysis of microRNA-203 function in CREB/MITF/RAB27a pathway: comparison between canine and human melanoma cells. Vet Comp Oncol 2016;14(4):384–94. https://doi.org/10.1111/vco.12118.
[36] Matišuk A, Rudij M, Rudij P. Human Thermohomeostasis onboard “MIR” and in simulated microgravity studies. Acta Astronaut 2001;11(1):109–31.
[37] Stahn AC, Werner A, Opatz O, Maggioni MA, Steinach M, Von Ahlefeld VW, et al. Increased core body temperature in astronauts during long-duration space missions. Sci Rep 2017;7(1):1–8. https://doi.org/10.1038/s41598-017-15560-w.
[38] Cox JF, Tahvanainen KUO, Kuusela TA, Levine BD, Cooke WH, Mano T, et al. Influence of microgravity on astronauts' sympathetic and vagal responses to Valsalva's manoeuvre. J Physiol 2002;538(Pt 1):309–20. https://doi.org/10.1113/jphysiol.2001.012574.
[39] Robinson EL, Fuller CA. Gravity and thermoregulation: metabolic changes and circadian rhythms. Pflueg Arch Eur J Physiol 2001;441(2–3 SUPPL):32–8. https://doi.org/10.1007/s004240000329.
[40] Dallas SL, Prideaux M, Bonewald LF. The osteocyte: an endocrine cell … and more. Endocr Rev 2013;34(5):658–90. https://doi.org/10.1210/er.2012-1026.
[41] Tian X, Jee WSS, Li X, Paszty C, Ke HZ. Sclerostin antibody increases bone mass by stimulating bone formation and inhibiting bone resorption in a hindlimb-immobilization rat model. Bone 2011;48(2):197–201. https://doi.org/10.1016/j.bone.2010.09.009.
[42] Frings-Meuthen P, Boehme G, Liphardt A-M, Baecker N, Heer M, Rittweger J. Sclerostin and DKK1 levels during 14 and 21 days of bed rest in healthy young men. J Musculoskelet Neuronal Interact 2013;13(1):45–52.
[43] Belavý DL, Baecker N, Armbrecht G, Beller G, Buehlmeier J, Frings-Meuthen P, et al. Serum sclerostin and DKK1 in relation to exercise against bone loss in experimental bed rest. J Bone Miner Metabol 2016;34(3):354–65. https://doi.org/10.1007/s00774-015-0681-3.
[44] Lin C, Jiang X, Dai Z, Guo X, Weng T, Wang J, et al. Sclerostin mediates bone response to mechanical unloading through antagonizing Wnt/beta-catenin signaling. J Bone Miner Res 2009;24(10):1651–61. https://doi.org/10.1359/jbmr.090411.
[45] Robling AG, Niziolek PJ, Baldridge LA, Condon KW, Allen MR, Alam I, et al. Mechanical stimulation of bone in vivo reduces osteocyte expression of Sost/sclerostin. J Biol Chem 2008;283(9):5866–75. https://doi.org/10.1074/jbc.M705092200.
[46] Morrell AE, Brown GN, Robinson ST, Sattler RL, Baik AD, Zhen G, et al. Mechanically induced Ca2+ oscillations in osteocytes release extracellular vesicles and enhance bone formation. Bone Research 2018;6(1):1–11. https://doi.org/10.1038/s41413-018-0007-x.
[47] Mullen M, Williams K, LaRocca T, Duke V, Hambright WS, Ravuri SK, et al. Mechanical strain drives exosome production, function, and miRNA cargo in C2C12 muscle progenitor cells. J Orthop Res 2023;41(6):1186–97. https://doi.org/10.1002/jor.25467.
[48] Uda Y, Azab E, Sun N, Shi C, Pajevic PD. Osteocyte mechanobiology. Curr Osteoporos Rep 2017;15(4):318–25. https://doi.org/10.1007/s11914-017-0373-0.
[49] Wang YY, Xia K, Wang ZX, Xie H, Xu R. Osteocyte exosomes accelerate benign prostatic hyperplasia development. Mol Cell Endocrinol 2021;531(December 2020):111301. https://doi.org/10.1016/j.mce.2021.111301.
[50] Motyl KJ, Bishop KA, DeMambro VE, Bornstein SA, Le P, Kawai M, et al. Altered thermogenesis and impaired bone remodeling in Misty mice. J Bone Miner Res 2013;28(9):1885–97. https://doi.org/10.1002/jbmr.1943.
[51] Nguyen AD, Lee NJ, Wee NKY, Zhang L, Enriquez RF, Khor EC, et al. Uncoupling protein-1 is protective of bone mass under mild cold stress conditions. Bone 2018;106:167–78. https://doi.org/10.1016/j.bone.2015.05.037.